

DYNAMIC MODELING AND ANALYSIS OF IN-WHEEL SUSPENDED ELECTRIC WHEEL SYSTEM

Peng Zhang*, Lei Jiang, ShangQing Liu, ShengShuo Yan, JingXin Bai, Ping Zhang

School of Mechanical Electronic and Information Engineering, China University of Mining and Technology-Beijing, Beijing 100083, China.

**Corresponding Author: Peng Zhang*

Abstract: The introduction of in-wheel motors increases the unsprung mass of electric vehicles, exacerbates vibrations when the vehicle is subjected to road excitation, and affects ride comfort and stability. The in-wheel suspended electric wheel has become an important technical means to improve the above-mentioned problems of in-wheel motors. This paper conducts a vertical dynamic characteristic analysis of two electric wheel configurations. A 1/4 vehicle model was established based on the Matlab/Simulink platform, and the vibration response characteristics of the two electric wheels under different road excitations were obtained. Experimental tests were performed on the vibration characteristics of the two electric wheels using a swept-sine road excitation. The experimental results were in good agreement with the simulation results, verifying the reliability and accuracy of the simulation model.

Keywords: In-wheel motor; Electric wheels; Internal suspension; Unsprung mass

1 INTRODUCTION

In-wheel motor (IWM) drive technology, which simplifies the powertrain system and enhances chassis layout flexibility, has become a key area in pure electric vehicle (EV) development. However, the integration of IWM significantly increases the unsprung mass of EV, leading to aggravated vertical vibrations under road excitation, which severely compromises ride comfort and handling stability [1]. This “negative unsprung mass effect” constitutes a major bottleneck hindering the widespread application of IWM drive technology. To address this issue, extensive research has been conducted on optimizing electric wheel configurations. The in-wheel suspended electric wheel, which integrates the motor into the wheel as a dynamic vibration absorber (DVA) via dedicated spring-damper mechanisms, effectively reduces the proportion of unsprung mass, offering a viable path to mitigate vibration problems. Current research has preliminarily validated the vibration improvement potential of suspended configurations. For instance, Rojas et al. compared the effects of passive, semi-active/active suspensions, and motor suspension devices on wheel dynamic load and body vibration acceleration, concluding that motor suspension significantly improves body vibration acceleration [2]. Chen et al. introduced a multifunctional integrated electric wheel structure with in-wheel suspension, which avoids the increase in unsprung mass [3]. Zhao et al. proposed a motor stator suspension scheme that transferred the motor stator mass to the sprung mass, resulting in body vertical vibration acceleration peaks comparable to those of centrally driven EV [4]. Li investigated the influence laws of the mass of mounting components in the dynamic vibration absorber and the mass of the motor as a part of the unsprung mass on the vertical dynamic performance of the vehicle, and obtained the optimal mass ranges of the two which were beneficial to the improvement of ride comfort [5]. Meng et al. studied a new type of electric wheel integrating a flexible transmission mechanism and a vibration damping mechanism. In this electric wheel, power transmission and vertical vibration were no longer coupled with each other, and could be designed or controlled separately, thus achieving favorable longitudinal and vertical dynamic characteristics of the vehicle [6]. However, existing studies often focus on single road conditions or localized performance optimization. Aiming to improve the vertical vibration performance of IWM-driven vehicles, this paper compares the vibration response characteristics of two electric wheel configurations under different road excitation and validates the simulation results through swept-sine excitation bench tests.

2 DYNAMIC MODELING OF THE ELECTRIC WHEEL SUSPENSION SYSTEM

2.1 Mathematical Model of the Electric Wheel

2.1.1 Mathematical model of the fixed in-wheel electric wheel

In most IWM-driven vehicles, the motor stator is fixed to the axle or steering knuckle arm through bearings, while the rotor is fixedly connected to the wheel rim. This configuration is termed the fixed in-wheel drive. The quarter-car model for the fixed in-wheel electric wheel suspension system is shown in Figure 1.

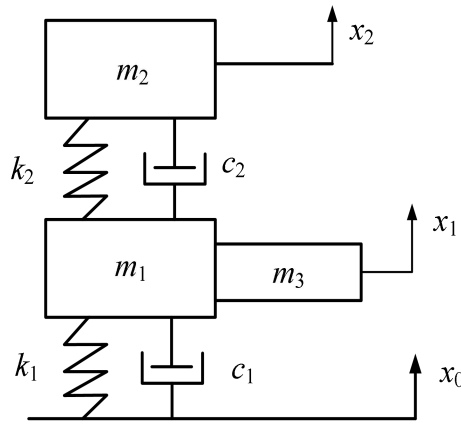


Figure 1 Quarter-Car Model of the Fixed In-Wheel Electric Wheel Suspension System

The vertical vibration differential equations for the fixed in-wheel vehicle are:

$$\begin{cases} (m_1 + m_3)\ddot{x}_1 + c_1(\dot{x}_1 - \dot{x}_0) + c_2(\dot{x}_1 - \dot{x}_2) + k_1(x_1 - x_0) + k_2(x_1 - x_2) = 0 \\ m_2\ddot{x}_2 + c_2(\dot{x}_2 - \dot{x}_1) + k_2(x_2 - x_1) = 0 \end{cases} \quad (1)$$

where m_1 is the unsprung mass excluding the IWM system; m_2 is the vehicle sprung mass; m_3 is the IWM system mass; k_1 and c_1 are the tire stiffness and damping; k_2 and c_2 are the suspension stiffness and damping; x_0 , x_1 , x_2 are the road excitation, wheel vertical displacement, and body vertical displacement, respectively.

2.1.2 Mathematical model of the in-wheel suspended electric wheel

The in-wheel suspended electric wheel connects the motor to the unsprung mass via dedicated springs and dampers, effectively utilizing the motor itself as a DVA. This structure significantly reduces the unsprung mass, making it comparable to conventional EV. Furthermore, by introducing dampers, the DVA effect is achieved without increasing the total vehicle mass, offering superior performance compared to traditional fixed in-wheel drive EV. The quarter-car model of the electric wheel suspension system based on the DVA is shown in Figure 2.

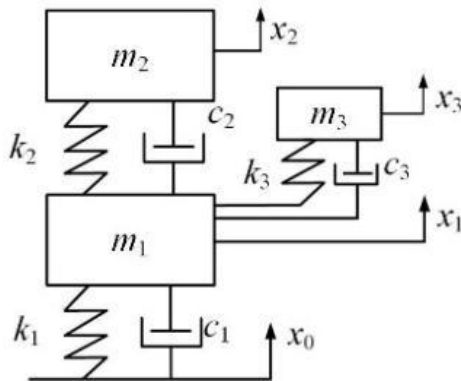


Figure 2 Quarter-Car Model of the In-Wheel Suspended Electric Wheel Suspension System

The vertical vibration dynamic equations for the in-wheel suspended vehicle are:

$$\begin{cases} m_1\ddot{x}_1 = k_1(x_0 - x_1) + c_1(\dot{x}_0 - \dot{x}_1) + k_2(x_2 - x_1) + c_2(\dot{x}_2 - \dot{x}_1) + k_3(x_3 - x_1) + c_3(\dot{x}_3 - \dot{x}_1) \\ m_2\ddot{x}_2 = k_2(x_1 - x_2) + c_2(\dot{x}_1 - \dot{x}_2) \\ m_3\ddot{x}_3 = k_3(x_1 - x_3) + c_3(\dot{x}_1 - \dot{x}_3) \end{cases} \quad (2)$$

where m_1 , m_2 , m_3 represent the unsprung mass, quarter-car sprung mass, and motor mass, respectively; k_1 , k_2 , k_3 represent the tire vertical stiffness, vehicle suspension stiffness, and motor DVA system stiffness, respectively; c_1 , c_2 , c_3 represent the tire vertical damping, vehicle suspension damping, and motor DVA system damping, respectively. x_0 denotes the road excitation, x_1 , x_2 , x_3 denote the vertical displacements of the respective masses.

2.2 Road Excitation Models

2.2.1 Random road

The random road model based on spectral analysis is a classical approach. Roads of different roughness levels are characterized by power spectral density (PSD) functions as input signals. The PSD of the road vertical velocity is calculated as follows:

$$G_q(f) = 4p^2 G_q(n_0) n_0^2 u \quad (3)$$

where $G_q(n_0)$ is the road PSD value at the reference spatial frequency $n_0=0.1\text{m}^{-1}$. This paper selects a Class E road surface with a roughness coefficient $G_q(n_0)=4.1\times 10^{-3}\text{m}^3$. The vehicle speed is $u=20\text{km/h}$.

2.2.2 Bump road

The bump road simulates obstacles such as speed bumps. The cross-section of a speed bump can be approximated by the cosine function over the interval $[-\pi/2, \pi/2]$. It is mathematically expressed as:

$$X_r = \begin{cases} \frac{1}{2}A \left[1 + \cos\left(2\pi \frac{L-L_0}{\lambda} - \pi\right) \right] & L_0 \leq L \leq L_0 + \lambda \\ 0 & \text{else} \end{cases} \quad (4)$$

where X_r is the vertical displacement (m), L is the vehicle travel distance (m), the bump height is $A=0.05\text{m}$, the bump length is $\lambda=0.25\text{m}$, and the distance from the starting point to the bump is $L_0=5\text{m}$.

2.2.3 Swept-sine road

Swept-sine excitation is commonly used in vibration studies. Since the natural frequencies of most vehicle bodies, seats, and wheels range from 0.7 Hz to 15 Hz [7], suspension research often employs swept-sine surfaces with linearly varying frequency [8]. It uses vibration spectra from typical road conditions to generate test excitation signals, simulating vibrations on different road surfaces.

The swept-sine road profile is calculated as:

$$X_r(L)=A \sin(\Omega L) \quad (5)$$

Where A is the road amplitude, $A=0.1\text{m}$; L is the vehicle travel distance (m); Ω is the angular spatial frequency of the sine road (rad/m). The vehicle speed increases from 10 m/s to 15 m/s with an acceleration of 1 m/s².

2.3 Performance Evaluation Metrics

To evaluate the vehicle's vertical dynamic characteristics, four metrics are selected: wheel vertical dynamic load, motor vertical vibration acceleration, body vertical acceleration, and body suspension dynamic deflection. The wheel vertical dynamic load represents the adhesion effect between the tire and the road. As the vertical dynamic load of the wheel decreases, the traction performance of the vehicle also decreases accordingly. The motor vertical vibration acceleration reflects the motor's vertical vibration amplitude. The body vertical acceleration indicates the vibration level experienced by the vehicle and its occupants. The body suspension dynamic deflection relates to the spatial requirements of the structure; a larger dynamic deflection increases the likelihood of suspension-contact with limit stops, implying reduced comfort. The calculation formulas are as follows:

$$\begin{cases} F_r = k_1(x_1 - x_0) + c_1(\dot{x}_1 - \dot{x}_0) \\ a_1 = \ddot{x}_2 \\ y = x_3 - x_1 \\ a_2 = \ddot{x}_3 \end{cases} \quad (6)$$

Where F_r is the wheel vertical dynamic load, a_1 is the motor vertical acceleration, y is the body suspension deflection, a_2 is the body vertical acceleration.

To reflect the vertical characteristics of the vehicle or motor at each frequency within the studied band, the relative amplitude-frequency characteristics of each metric are used for evaluation, the calculation formula is as follows:

$$\begin{cases} J_1 = \frac{\left| \widehat{F_r} \right|}{\left| G \widehat{\dot{x}_0} \right|} \\ J_2 = \frac{\left| \widehat{\ddot{x}_2} \right|}{\left| \widehat{\dot{x}_0} \right|} \\ J_3 = \frac{\left| \widehat{x_1 - x_3} \right|}{\left| \widehat{\dot{x}_0} \right|} \\ J_4 = \frac{\left| \widehat{\ddot{x}_1} \right|}{\left| \widehat{\dot{x}_0} \right|} \end{cases} \quad (7)$$

where G is the total weight of the quarter-car; J_1 、 J_2 、 J_3 、 J_4 represent the relative amplitude-frequency characteristics of wheel dynamic load, motor vertical acceleration, body suspension dynamic deflection, and body vertical acceleration under road excitation, respectively. “ \wedge ” denotes the Laplace transform.

3 SIMULATION RESULTS AND ANALYSIS

The specific parameters for the in-wheel suspended and fixed configurations are shown in Table 1. A corresponding quarter-car model was established in Matlab/Simulink. Road excitations were applied to the model to simulate vibration response characteristics under different conditions.

Table 1 Simulation Parameters

Parameter Symbol	In-Wheel	Suspended	Fixed	Parameter Symbol	In-Wheel	Suspended	Fixed
m_1 (kg)	40	40		k_2 (N/m)	32000	32000	
m_2 (kg)	340	340		c_2 (N·s/m)	1496	1496	
m_3 (kg)	30	30		k_3 (N/m)	41000		
k_1 (N/m)	360000	360000		c_3 (N·s/m)	1000		
c_1 (N·s/m)	50	50					

3.1 Simulation Analysis Under Random Road Excitation

Setting the random road excitation, the time-domain comparisons of various vehicle performance metrics are shown in Figure 3.

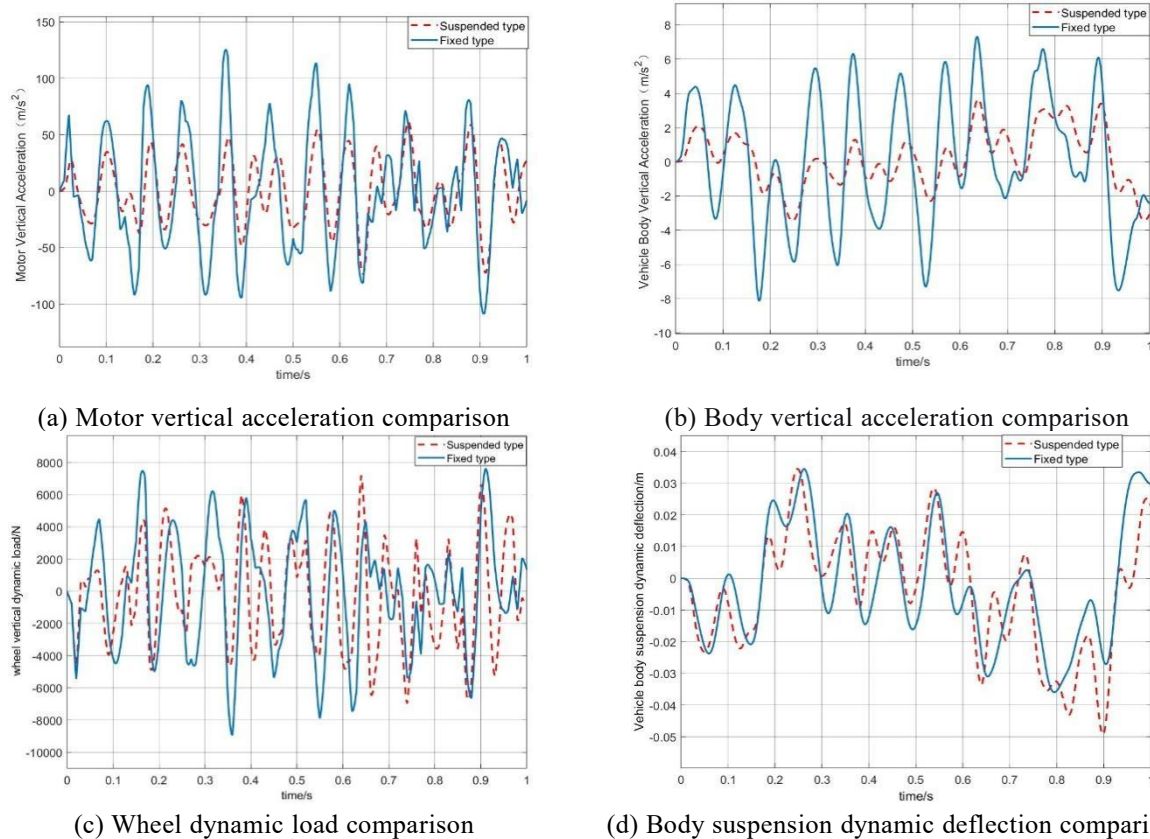
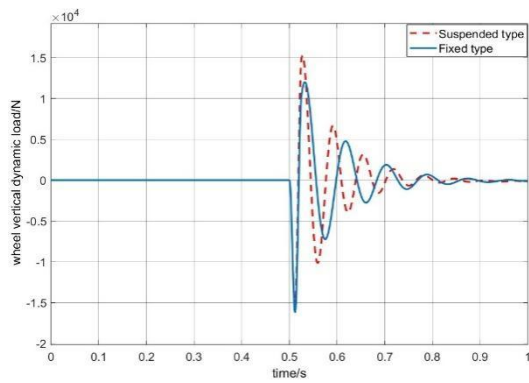


Figure 3 Time-Domain Comparison of Performance Metrics under Random Road Excitation

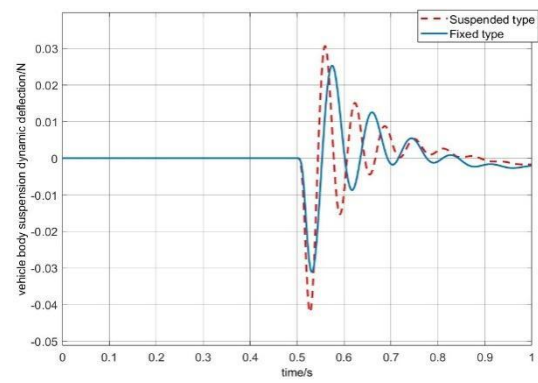
As shown in Figure 3, the in-wheel suspended configuration effectively reduces the vertical vibration of the IWM. Compared to the fixed configuration, the in-wheel suspended motor reduces body vibration levels, thereby improving passenger comfort. The amplitude of the wheel vertical dynamic load for the in-wheel suspended configuration is significantly smaller than that of the fixed configuration, indicating better adhesion between the tire and road, and consequently better traction performance. The body suspension dynamic deflection of the in-wheel suspended configuration is similar to that of the fixed configuration. And it is even larger than the fixed configuration's deflection between 0.8s and 0.9s. This suggests that the increased unsprung mass due to placing the motor inside the wheel is not fully mitigated by suspending the motor, and the issue of potential suspension-contact with limit stops persists.

3.2 Simulation Analysis Under Bump Road Excitation

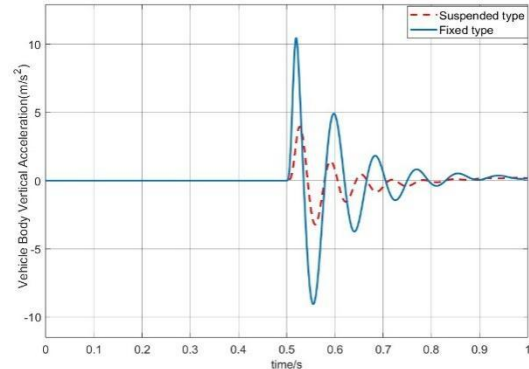
Setting the bump road excitation, the time-domain comparisons of various performance metrics are shown in Figure 4.



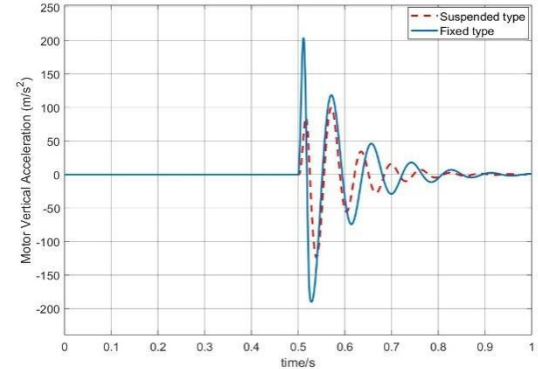
(a) Wheel dynamic load comparison



(b) Body suspension dynamic deflection comparison



(c) Body vertical acceleration comparison



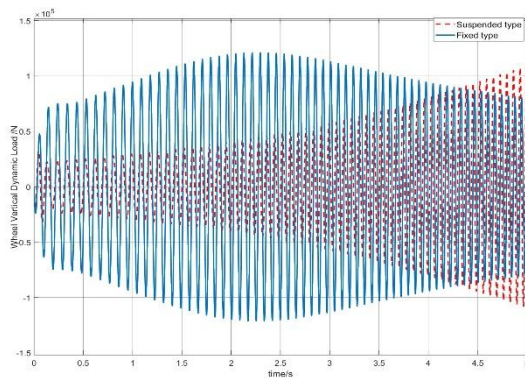
(d) Motor vertical acceleration comparison

Figure 4 Time-Domain Comparison of Performance Metrics under Bump Road Excitation

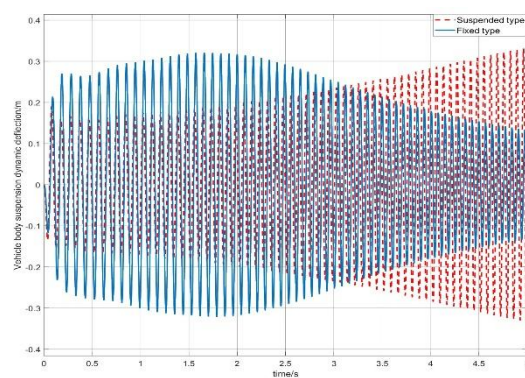
As shown in Figure 4, the wheel dynamic load and body suspension dynamic deflection of the in-wheel suspended electric vehicle are slightly larger than those of the fixed electric vehicle, but the difference is minimal when traversing a bump road. This indicates that suspending the in-wheel motor doesn't significantly enhance tire-road adhesion or reduce the likelihood of suspension collision on bumpy roads. However, the body vertical acceleration and motor vertical acceleration of the in-wheel suspended electric vehicle are smaller than those of the fixed configuration, suggesting that passengers experience lower vibration amplitudes in the suspended configuration, meaning that the comfort level has been improved.

3.3 Simulation Analysis Under Swept-Sine Excitation

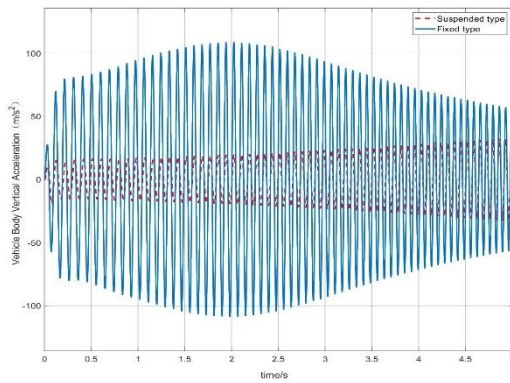
Setting the swept-sine road excitation, the time-domain comparisons of various performance metrics are shown in Figure 5.



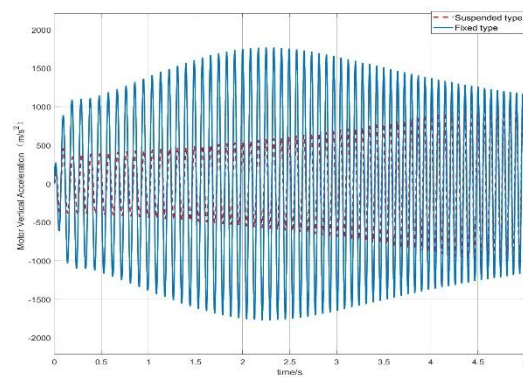
(a) Wheel dynamic load comparison



(b) Body suspension dynamic deflection comparison



(c) Body vertical acceleration comparison



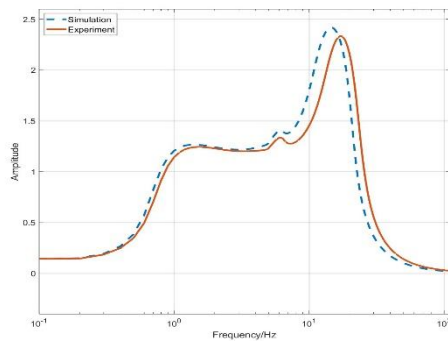
(d) Motor vertical acceleration comparison

Figure 5 Time-Domain Comparison of Performance Metrics under Swept-Sine Road Excitation

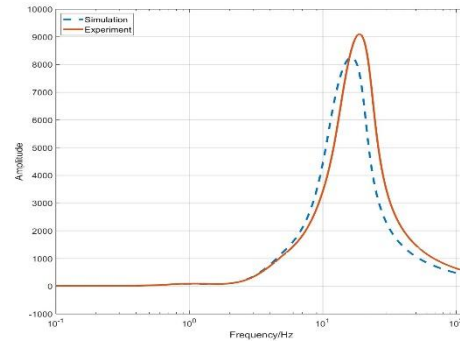
As shown in Figure 5, the wheel dynamic load and body suspension dynamic deflection are related to vehicle speed. On a fixed-frequency sine road, the in-wheel suspended configuration exhibits larger wheel dynamic load and body suspension deflection than the fixed configuration after vehicle speeds exceed 14 m/s and 13 m/s, respectively. This indicates that at lower speeds, the in-wheel suspended configuration can effectively reduce wheel dynamic load and body suspension deflection, enhancing road-holding ability and reducing the likelihood of suspension collision. However, this improvement diminishes and may even become worse than the fixed configuration at higher speeds. In contrast, the improvement in body vertical acceleration and motor vertical acceleration for the in-wheel suspended configuration doesn't deteriorate with increasing speed.

4 EXPERIMENTAL VALIDATION AND COMPARATIVE ANALYSIS

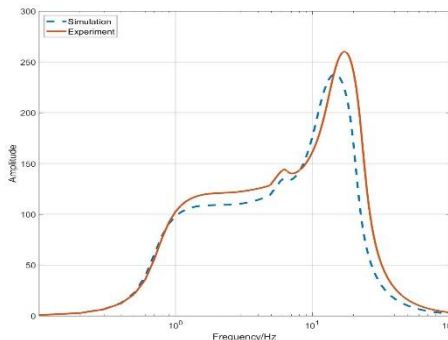
The complexity and strong randomness of actual road conditions pose significant challenges for quantitative analysis. To validate the effectiveness of the dynamic model for the in-wheel suspended electric wheel, this experiment and simulation comparison selected swept-sine road excitation as the unified condition. This excitation covers the main vibration frequency bands encountered in actual vehicle operation through continuously varying frequency and maintains consistent parameters with the simulation phase, comprehensively reflecting the system's vertical dynamic response at different frequencies. The amplitude-frequency diagrams of acceleration outputs from various parts for both test and simulation are shown in Figure 6.



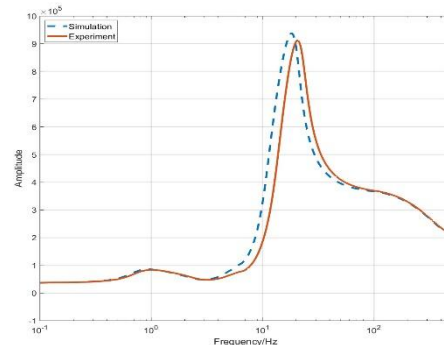
(a) The suspension dynamic deflection



(b) The motor vertical acceleration



(c) The body vertical acceleration



(d) The wheel dynamic load

Figure 6 Comparison of Frequency Response Curves between Test and Simulation for Various Metrics under Swept-Sine Road Excitation

Analysis of the amplitude-frequency characteristic curves above reveals that for the in-wheel suspended configuration, the overall fluctuation amplitudes of the experimental and simulated amplitude-frequency curves for wheel, motor, and body vertical acceleration are relatively close. At lower frequencies, the experimental and simulation results are nearly identical. As speed increases, deviations gradually appear between experiment and simulation. This is due to the difficulty in accurately determining the stiffness and damping coefficients of the body suspension and motor suspension springs/dampers in the actual experiment, leading to discrepancies. However, the results are generally in good agreement, indicating the correctness of the simulation model.

5 CONCLUSIONS

Mathematical models based on mass-spring-damper systems were established for both fixed and in-wheel suspended electric wheel systems. Wheel vertical dynamic load, motor vertical vibration acceleration, body vertical acceleration, and body suspension deflection were identified as vehicle performance evaluation metrics. Random road, bump road, and swept-sine road models were constructed.

The dynamic characteristics were analyzed based on time-domain plots of the four metrics under random, bump, and swept-sine road excitations. It was concluded that the in-wheel suspended configuration improves vehicle vertical vibration performance and ride comfort compared to the fixed configuration. However, the suspended configuration's ability to improve wheel dynamic load and body suspension deflection is influenced by vehicle speed, while its improvement in body and motor vertical acceleration is not affected by speed.

Using swept-sine excitation as input, amplitude-frequency characteristic curves for wheel, motor, and body vertical acceleration were obtained experimentally. And the amplitude-frequency characteristic curves from road excitation to wheel dynamic load, body suspension deflection, and the aforementioned accelerations were derived. Comparison between experimental and simulation results further verified the reliability of the simulation model.

COMPETING INTERESTS

The authors have no relevant financial or non-financial interests to disclose.

FUNDING

This study was supported by National Training Program of Innovation and Entrepreneurship for Undergraduates (Project No.202513038) and Fundamental Research Funds for the Central Universities.

REFERENCES

- [1] Ning GB, Wan G. Research status of the influence of wheel-side drive system on vehicle vertical performance. *Automobile Technology*, 2007, 3: 21-25.
- [2] Rojas AER, Niederkofler H, Willberger J. Comfort and safety enhancement of passenger vehicles with in-wheel motors. *Society of Automotive Engineers*, 2010, 1-12.
- [3] Chen C, Cheng Y, Meng F. Optimum design of a novel in-wheel suspension of the electric wheel. *IEEE 3rd International Conference on Green Energy and Applications*, 2019: 3-10.
- [4] Zhao YE, Zhang JW, Han X. Design and research on dynamic vibration reduction mechanism of in-wheel motor independent drive electric vehicle. *Mechanical Science and Technology*, 2008, 3: 3-4.
- [5] Li G. Research on ride comfort of mounting configuration for in-wheel motor driven electric vehicles. Qingdao: Shandong University of Science and Technology, 2020.
- [6] Meng L, Qin Y, Zou Y, et al. A new type of hub-driven electric wheel and its vertical vibration analysis. *Proceedings of 2019 SAE-China Congress & Exhibition*, 2019, 2: 1-2.
- [7] Wei W. Design and control strategy of electromagnetic active suspension. Shenyang: Shenyang University of Technology, 2020.
- [8] Nie SD. Research on comprehensive performance of semi-active suspension considering fixed point characteristics. Changchun: Jilin University, 2018.